

## Biphasic Chemokinesis of Mammalian Sperm

Meisam Zaferani<sup>1</sup> and Alireza Abbaspourrad<sup>1\*</sup>*Department of Food Science, Cornell University, Ithaca 14850, New York, USA* (Received 31 May 2022; accepted 3 April 2023; published 12 June 2023)

The female reproductive tract (FRT) continuously modulates mammalian sperm motion by releasing various clues as sperm migrate toward the fertilization site. An existing gap in our understanding of sperm migration within the FRT is a quantitative picture of how sperm respond to and navigate the biochemical clues within the FRT. In this experimental study, we have found that in response to biochemical clues, mammalian sperm display two distinct chemokinetic behaviors which are dependent upon the rheological properties of the media: chiral, characterized by swimming in circles; and hyperactive, characterized by random reorientation events. We used minimal theoretical modeling, along with statistical characterization of the chiral and hyperactive trajectories, to show that the effective diffusivity of these motion phases decreases with increasing concentration of chemical stimulant. In the context of navigation this concentration dependent chemokinesis suggests that the chiral or hyperactive motion refines the sperm search area within different FRT functional regions. Further, the ability to switch between phases indicates that sperm may use various stochastic navigational strategies, such as run and tumble or intermittent search, within the fluctuating and spatially heterogeneous environment of the FRT.

DOI: [10.1103/PhysRevLett.130.248401](https://doi.org/10.1103/PhysRevLett.130.248401)

Searching for targets within complex biological environments requires efficient migration strategies. To appropriately migrate in complex settings, searchers must obtain exogenous clues from the environment and regulate their motion according to the information provided [1]. At the microscopic scale, examples include canonical bacterial chemotaxis in fluctuating environments [2–5], T-cell locomotion in tissues [6–9], and mammalian sperm migration within the female reproductive tract (FRT) [10]. Sperm migration within the FRT, however, is unique; they travel  $\sim 10^3 - 10^5$  times their own length and throughout their journey they are subjected to an intense selection process [11,12] designed to find the most competent among the billions of sperm deposited. Furthermore, unlike bacteria and somatic cells, sperm nuclei are mostly inactive [13], which makes their performance heavily reliant upon the FRT. Such strong dependence upon the FRT, is a potential driving force for the evolution of sperm morphology, which is known to be shaped by form of the FRT [14]. In the context of navigation, it is widely thought that the FRT steers sperm toward the oocyte using physiological factors. This is a multistep process constantly regulated by the FRT which releases clues that sperm respond to and then use to navigate to their target.

The biophysical clues that actively modulate mammalian sperm motion have been identified as the rheological properties [15,16] and flow of mucus [17–22] within the FRT, and the physical boundaries of the FRT [23–27]. How mammalian sperm respond to the biochemical clues released in the FRT, is the current question. In marine animals where fertilization occurs externally, it has been

well documented that the biochemical stimulus near the oocyte regulates sperm motion and promotes a relatively deterministic chemotactic behavior [28,29]. However, less is known for mammals where fertilization occurs within the FRT, and the sperm motion regulating biochemicals originate at distances far from the target oocyte [28]. That these clues originate at a distance, highlights that chemokinetic effects triggered by the FRT contribute continuously to the sperm navigation and are not limited to the final stages of fertilization. Such a response is likely to promote stochastic navigational strategies, as opposed to a deterministic chemotaxis, to benefit the search for the remote oocyte.

Extensive studies have revealed the sperm chemokinetic response to biochemicals released from the FRT through activation of the pH-sensitive CatSper channels on its flagellum. When activated, the resulting increase in cytoplasmic  $\text{Ca}^{2+}$  concentration modulates sperm flagellar beating patterns and causes a reversible chemokinetic response known as “hyperactivation” [28–39]. Although hyperactivation induced modulation of flagellar beating patterns and its resulting physiological significance has been studied [33–36], a statistical picture of hyperactivation at the single-cell trajectory level elucidating the role of chemokinesis in promoting possible stochastic navigational strategies remains to be developed.

We explored bull sperm motion within quiescent circular microfluidic chambers with two parallel surfaces to establish a quantitative connection between hyperactivation and its function in sperm navigation within the FRT. We present statistical characterization of single cell trajectories in viscous and viscoelastic media at various levels of biochemical

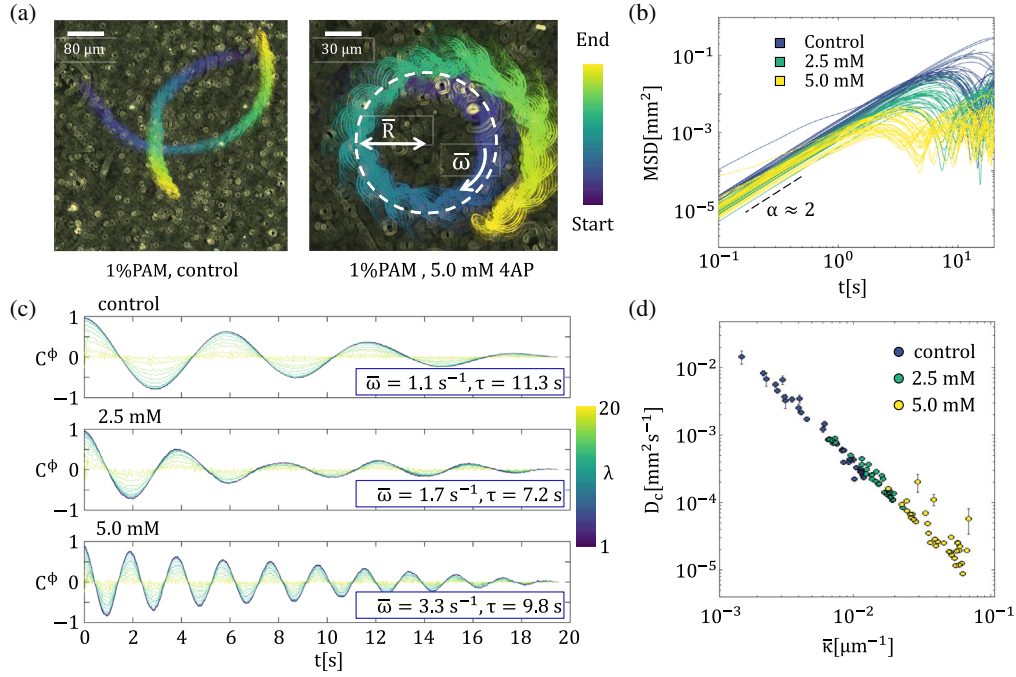


FIG. 1. Experimental characterization of sperm chiral motion. (a) Left: overlaid images acquired from the chiral motion in 5 seconds (frame rate  $\sim 25$  frame/s). Right: overlaid images acquired from the 4AP treated chiral motion in 5 seconds (frame rate  $\sim 25$  frame/s). (b) MSD of chiral motion (35 trajectories for each treatment). (c) Orientational autocorrelation of the chiral motion, with and without treatments.  $\lambda$  is a coarse graining parameter (Fig. S2 [41]). (d) Effective diffusivity of the chiral motion vs the curvature of the circular path.

stimulation. We show that depending on the rheological properties of the media, sperm exhibit distinct tunable chemokinetic responses: chiral motion, with swimming on circular patterns; or hyperactive motion characterized by random reorientations. Modeling the stochastic dynamics of chiral and hyperactive phases, we further discuss the consequences of our findings and justify how such tunable chemokinetic responses allow sperm to exhibit stochastic navigational strategies in the fluctuating environment of the FRT.

*Experimental setup.*—Throughout this Letter, we observed sperm motion in microfluidic Hele-Shaw chambers (diameter =  $600 \mu\text{m}$  and height  $h \approx 30 \mu\text{m}$ ) using phase contrast microscopy. We chose this geometry because it represents the generic narrow quasi-two-dimensional passages of the FRT [40]. After recording sperm motion (25 frames/s) and tracking its centroid, we coarse grained the acquired trajectories to remove the short-time fluctuations caused by the rapid oscillations of the sperm body. Without coarse graining, such rapid oscillations dominated our measurement and long-term swimming behaviors were not discernible. Detailed information about our experimental setup is available in Supplemental Material, Methods [41].

*Chiral motion.*—In agreement with our previous report, we observed that in a viscoelastic media such as standard Tyrode’s albumin lactate pyruvate (TALP [19]) buffer

medium plus 1% polyacrylamide (PAM), sperm motility is solely two-dimensional (2D) flagellar beating with no rolling around their longitudinal axes. The intrinsic asymmetry associated with flagellar beating resulted in a 2D chiral motion with low rotational speed (Fig. S1 [41]), such that sperm swim in circular trajectories [Fig. 1(a)]. The mean radii of these circular trajectories do not change significantly over time and are  $\sim 3$ – $20$  times greater than sperm length (Supplemental Material, Fig. S1 [41]). While we observed that chiral motion featured both clockwise and counterclockwise handedness in a sperm population, we did not observe a change in the handedness of each individual sperm. Measuring the corresponding mean square displacement (MSD), we found that transition from ballistic motion ( $\alpha \approx 2$ ) at short timescales to chiral motion appeared in  $\sim 10$  s [Fig. 1(b)] with significant variations among sperm within the population; some sperm with low curvatures in their circular paths remained in the ballistic regime for the whole period of observation.

To explore how chemokinetic factors regulate sperm chiral motion, we treated sperm with 4-aminopyridine (4AP) [42], an established hyperactivation inducer. 4-AP is a potassium channel antagonist that most likely activates the CatSper channel by increasing sperm cytoplasmic pH [40]. Activation of CatSper channel and the subsequent rise in  $\text{Ca}^{2+}$  concentration most likely results in regulation of the flagellar dynein motors activity via calmodulin

(a calcium sensitive protein) and consequently leads to more asymmetry in the flagellar beating pattern [43]. We found that the addition of 2.5 and 5.0 mM of 4AP to a 1% PAM solution increased the curvature of the circular path in chiral motion ( $\bar{\kappa} = \bar{R}^{-1}$ ) significantly [Fig. 1(a) and Fig. S1, Movie S2 [41]]. This increase in curvature was caused by an increase in the flagellar asymmetry and thus the net rotational speed ( $\bar{\omega}$ ) of the chiral motion (Fig. S1 [41]). Notably, this change is concentration dependent and when 5 mM 4AP was used, the increase in the curvature was so strong that the chiral surface explorations became intensive exploitations on tight circles with radii close to the sperm length [Fig. 1(a)]. Furthermore, 4AP treatments reduced the curvature variations among sperm within the population and shortened the transition time from ballistic to the chiral phase [MSD in Fig. 1(b)]. We noted that handedness of the chiral phase in 4AP treated sperm did not change during our observations.

To quantify the chiral phase and its regulation via 4AP, we modeled this phase using the following stochastic differential equations:

$$\dot{\vec{r}} = \bar{u} \hat{e}, \quad (1a)$$

$$\dot{\phi} = \bar{\omega} + \sqrt{2D_\phi} \varepsilon(t), \quad (1b)$$

where  $\bar{u}$  is the sperm net translational speed,  $\hat{e}$  is a unit vector representing the sperm orientation,  $\{\varepsilon(t)\}$  is white Gaussian noise, and  $D_\phi$  is the corresponding rotational diffusivity. The noise term is dominated by active flagellar fluctuations and imprecision in chemical sensing, rather than thermal fluctuations [44]. We neglected the fluctuations in the sperm speed as they do not induce a drift in the trajectory [45]. Consequently, the orientational auto-correlation is

$$C_\phi(t) = \langle \hat{e}(t') \cdot \hat{e}(t' + t) \rangle = \cos(\bar{\omega}t) \exp(-t/\tau), \quad (2)$$

in which,  $\tau$  is the relaxation time  $D_\phi = \tau^{-1}$  and  $\langle \dots \rangle$  denotes average over the ensemble of stochastic trajectories. Accordingly, the effective diffusivity [46–48] (Supplemental Material, Theory [41]) can be written as

$$D_C = \frac{1}{2} \int_0^\infty dt \langle \dot{\vec{r}}(0) \cdot \dot{\vec{r}}(t) \rangle = \frac{1}{2} \int_0^\infty dt \bar{u}^2 C_\phi(t) = \frac{\bar{u}^2}{2} \left( \frac{D_\phi}{D_\phi^2 + \bar{\omega}^2} \right). \quad (3)$$

Measuring  $C_\phi$  for the control and the 4AP treated sperm [three representative sperm are shown in Fig. 1(c)] and fitting the right-hand side of Eq. (2) to the experimental results, we measured  $\bar{\omega}$ ,  $\tau$  and thus infer the effective diffusivity via Eq. (3) for each individual sperm [Fig. 1(d)]. Our measurements indicate that the effective diffusivity of the chiral phase decreases with 4AP treatments: not only

does the circle become smaller, but it also becomes more localized. This localization was primarily due to an increase in the curvature of the circular path [correlation coefficient ( $\gamma$ )  $\approx -0.99$ ], rather than changes in the rotational diffusivity. Furthermore, the variation of effective diffusivity among sperm in the population decreased with the 4AP treatments.

*Hyperactive motion.*—In Newtonian fluids with low viscosities like TALP (without PAM), we observed that bull sperm motility consists of flagellar beating as well as frequent rolling around the longitudinal axis [49–51] [Fig. 2(a) box, frequency =  $7.1 \pm 2.5$  Hz according to Ref. [40]] which allows them to move progressively forward in straight lines. We observed this rolling component under a phase contrast microscope; the light intensity of the sperm head appears to flash with every incidence of rolling [Fig. 2(a), box]. Previously we showed that, while flagellar beating propels sperm forward, the rolling component neutralizes the effect of intrinsic asymmetry and keeps the sperm moving persistently in a straight line [Fig. 1(a)]. However, upon entry into a viscoelastic fluid, this rolling component becomes suppressed, and this progressive motion reversibly transitions into chiral motion. Although the mechanism behind this rolling suppression in non-Newtonian fluids is yet to be further investigated, based on recent findings on suppression of bacterial wobbling in complex fluids [52], we speculate that a physical model incorporating the colloidal nature of complex fluids might explain suppression of sperm rolling in our polymeric solutions. Sperm progressive motion which is sensitive to external fluid flows and nearby physical boundaries like walls of the FRT, has been studied extensively in the past in various contexts [17,18,23,24,26,27,53].

To investigate how this progressive motion was further modulated by 4AP, we added 2.5 and 5.0 mM of 4AP to the TALP solution without PAM. We observed that the trajectories of sperm treated with 2.5 and 5.0 mM of 4AP deviate from straight lines [Fig. 2(a), and Supplemental Material, Movie S3 [41]]. These trajectories are reminiscent of the persistent random walks observed for active colloidal particles [54] and droplets [55,56]. We measured the translational speed of the 4AP treated sperm [Fig. 2(a)] and found a significant decrease in the sperm translational speed after treatments. The fluctuations in the speed (except for sharp reorientation events) were either below our experimental error ( $\pm 5 \mu\text{m s}^{-1}$ ) or had short autocorrelation times. We measured the reorientation angle ( $\phi$ ) for 4AP treated sperm and found that the corresponding probability distributions widened as we increased the concentration of the drug [Fig. 2(b)]. This broadening in the distribution corresponds to more frequent and wider reorientations at 5.0 mM 4AP treatments where a sharp reorientation was defined as  $|\phi| > \pm(\pi/2)$ . We also measured the MSD [Fig. 2(c)] and found that 4AP treated sperm display as a “hyperactive phase” of motion which exhibits transition from ballistic at

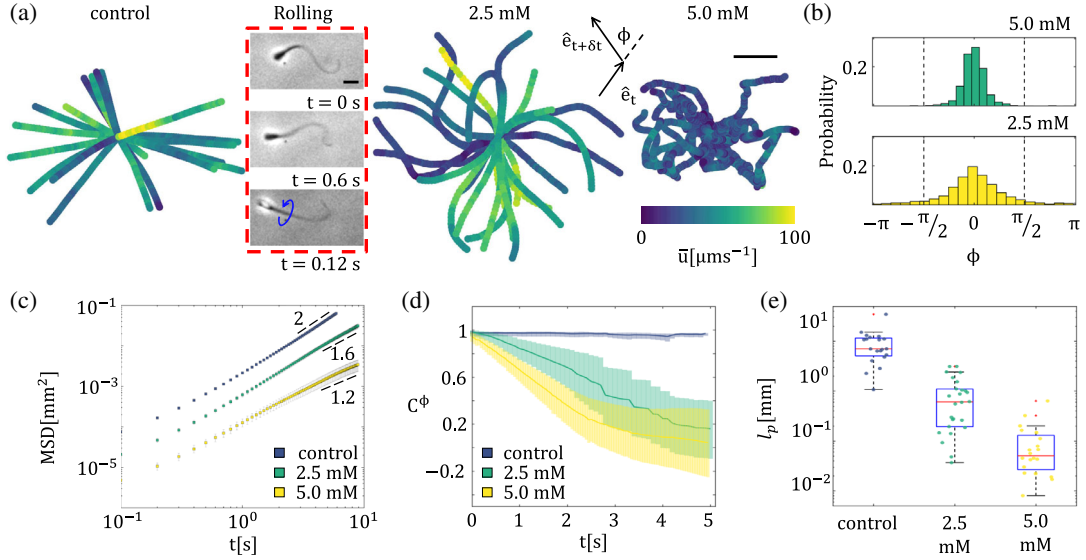


FIG. 2. Experimental characterization of sperm hyperactive motion. (a) Sperm trajectories at treatments with 2.5 and 5.0 mM of 4AP. The average time between points is  $\sim 0.08$ – $0.1$  s and trajectories are color coded according to the translational speed (scale on the top right:  $100 \mu\text{m}$ ). Box: sperm rolling (scale:  $10 \mu\text{m}$ ). (b) Probability distribution of reorientation angles. (c) MSD, (d) orientational autocorrelations, and (e) persistent length measured for the hyperactive phase. (25 trajectories for control and each treatment and \* $p$  value  $< 0.0001$ ).

short times to diffusive behavior ( $\alpha = 1$ ) at long times with decreasing power-law coefficient at intermediate timescales ( $\alpha = 1.6$  at 2.5 mM and  $\alpha = 1.2$  at 5.0 mM treatments).

To quantify the hyperactive phase, we measured the orientational autocorrelation for 4AP treated sperm and observed an exponential decay,  $C_\phi = \exp(-t/\tau)$  [Fig. 2(d)]. The large error bars indicate variations between sperm within a population. Measuring relaxation time ( $\tau$ ) and persistent length ( $l_p = \bar{u}\tau$ ) for each individual sperm [Fig. 2(e)], we characterized the loss of directionality that increased with 4AP treatments.

Because 4AP modulates asymmetry in flagellar beating, but does not modulate rolling (frequency =  $7.1 \pm 2.4$  Hz at 3 mM 4AP and  $7.6 \pm 2.9$  Hz at 5 mM with  $p$  value  $> 0.4$  according to Ref. [40]), we modeled the hyperactive phase as a chiral motion, in which the direction of rotational speed ( $\bar{\omega}$ ) reverses independently with every rolling. That said, we included the effect of rolling by adding  $\Pi(t)$  as a coefficient to Eq. (1b):

$$\dot{\phi} = \Pi(t)\bar{\omega} + \sqrt{2D_\phi}\epsilon(t). \quad (4)$$

$\{\Pi(t)\}$  is a continuous-time Markov process that alternates randomly between  $\pm 1$  values with every rolling. This coefficient captures the counteractive effect of rolling on the asymmetry in the flagellar beating, as the ensemble average of sperm reorientation becomes vanishingly small ( $\langle \phi \rangle \approx 0$ ) while the variance is

$$\langle \phi(t)^2 \rangle = \bar{\omega}^2 \int_0^t dt' \int_0^{t'} dt'' C_\Pi(t' - t'') + 2D_\phi t, \quad (5)$$

in which  $C_\Pi(t' - t'') = \langle \Pi(t') \cdot \Pi(t'') \rangle$  is the autocorrelation of rolling and has an exponential form  $C_\Pi(t' - t'') = \exp[-(2|t' - t''|)/\langle T \rangle]$ , with  $\langle T \rangle$  being the average time between two consecutive rolling events (Supplemental Material, Theory [41]). For timescales much longer than the autocorrelation time, the variance is approximately

$$\langle \phi(t)^2 \rangle \approx (\bar{\omega}^2 \langle T \rangle + 2D_\phi)t, \quad (6)$$

and the orientational autocorrelation can be written as  $C_\phi(t) = \exp(-D_\phi^* t)$ . Therefore, the hyperactive phase is a persistent random walk whose rotational diffusivity ( $D_\phi^*$ ) is coupled with the sperm rotational speed and average time between two rolling events [Eq. (7)]:

$$D_\phi^* \approx D_\phi + \frac{1}{2}\bar{\omega}^2 \langle T \rangle. \quad (7)$$

As the chemical stimulation increases the asymmetry in the flagellar beating, and thus rotational speed, it also contributes to the rotational diffusivity and tunes the persistent length. The persistent random walk description also predicts that MSD of the hyperactive phase as [57]

$$\text{MSD} = \frac{2\bar{u}^2}{D_\phi^*} \left[ t + \frac{e^{-D_\phi^* t} - 1}{D_\phi^*} \right]. \quad (8)$$

Equation (8) agrees with the transition from ballistic into diffusive behavior observed for the hyperactive phase and further suggest the effective diffusivity of  $D_H = \bar{u}^2/2D_\phi^*$  (Fig. S3 [41]). Because the transition into the diffusive

behavior becomes faster with the increase of  $D_{\phi}^*$  (coupled with  $\bar{\omega}$ ), our model also explains the faster transition into diffusive behavior observed at treatments with higher concentrations of 4AP (Fig. S3). Based on our measurements of translational speed and rotational diffusivity, we inferred the effective diffusivity of the hyperactive phase [Fig. 3(a)] for 4AP treated sperm and found that at higher doses of 4AP, we observed lower effective diffusivities. However, such a decrease in the effective diffusivity cannot be solely attributed to the decrease in the translational speed ( $\gamma \approx 0.84$ ), because in contrast to the chiral phase, 4AP contributes significantly to the modulation of the rotational diffusivity of the hyperactive phase.

Random reorientations observed in the hyperactive phase also modulate sperm-wall interactions as previously reported [40], and high levels of hyperactivation (5.0 mM 4AP) resulted in detachments from the sidewall of our microfluidic chamber [Fig. 3(b), and Supplemental Material, Movie S4 [41]]. These escapes from the wall potential (marked by “a” and “b”) were caused by sharp reorientations ( $|\phi| > \pi/2$ ) in sperm trajectory [Fig. 3(c)].

*Discussion.*—But how does the observed tunable chemokinetic behavior enable sperm to migrate within the FRT at far distances from the oocyte? At low concentration of biochemical stimuli, both progressive and chiral motion are, respectively, suitable for directed migration over long distances and exploring large viscoelastic areas [Fig. 3(d)].

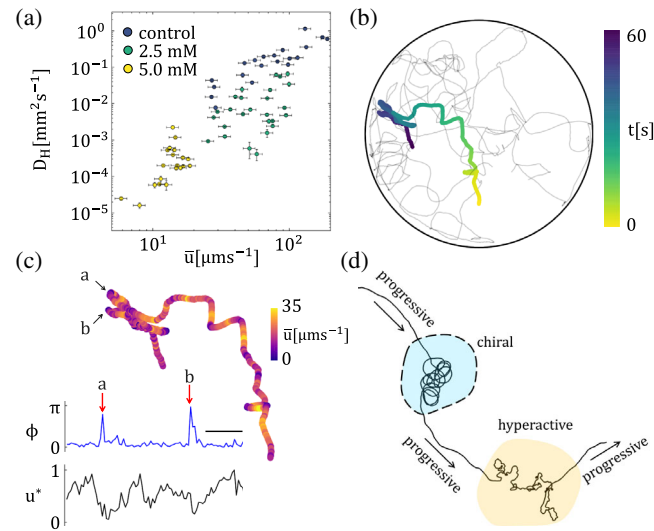


FIG. 3. (a) Effective diffusivity of the hyperactive phase vs translational speed. (b) Sperm treated with 5.0 mM 4AP exhibited detachments from the sidewall. One of the trajectories is color coded according to elapsed time. Diameter of chamber: 600  $\mu\text{m}$ . (c) Same trajectory is color coded according to translational speed.  $\phi$  is the reorientation angle and  $u^*$  is the normalized translational speed. Detachments from sidewall are marked with “a” and “b”. These detachments are caused by sharp reorientation events. Scale bar: 5 s. (d) Picture of sperm motion including progressive, chiral, and hyperactive phases.

As the concentration of stimuli increase, the progressive motion transitions into the hyperactive phase with a tunable persistence length, and the chiral phase becomes more localized with tunable diffusivity to encourage exploitation of nearby regions. Such tunable chemokinetic behaviors are potentially needed within the tract to decrease the search area and increase the probability to find the source of the biochemical stimuli.

Further, our results suggest that sperm chemokinesis can function as the basis for stochastic navigational strategies, such as run and tumble within the FRT, where the fixed orientation of sperm progressive motion is altered by transient chiral or hyperactive motions that are induced by local increases in biochemical stimuli [Fig. 3(d)]. We expect that more frequent biochemical stimulations at higher intensities would result in more frequent tumbling in fluctuating environments. On a broader perspective, biphasic chemokinesis, the combined effect of biochemicals and ambient rheology, may also cause sperm to perform intermittent behaviors [47,58,59] with random transitions within the fluctuating and spatially heterogenous environment of FRT. While the function of stochastic navigation promoted by chemokinesis is, in general, attributed to the search for the oocyte, sperm migration within the FRT is a multistep process and other essential physiological factors must be delivered to the sperm before they reach to the oocyte. Since the chemokinetic response can be induced independent of the oocyte, we argue that stochastic navigation can also contribute to the search for other physiological targets that are essential for the fertilization.

In the context of stochastic navigation, hyperactive and chiral phase seem to play similar functions: reducing the effective diffusivity and frequently changing the swimming direction. Despite these similarities, sharp reorientations observed during hyperactivity increase the sperm’s ability to escape from the wall potential, which enables sperm to perform stochastic navigation in the complex architecture of the FRT and pass through it without becoming trapped. Note that the progressive and chiral phases of motion lack sharp reorientation events and thus are vulnerable to becoming trapped by architectural confinements [60]. Further, unlike the hyperactive phase, sperm in the chiral phase can potentially receive additional directional guidance in a chemical gradient created by the nearby oocyte and swim in circular trajectory such that they drift deterministically toward the oocyte [61]. These functional differences between hyperactive and chiral phases highlight the significance of sperm biphasic chemokinesis in the FRT.

In our study, we either observed sperm exhibiting frequent rolling in Newtonian fluids, or full suppression of rolling in polymeric solutions. However, we speculate that in a swimming media with heterogeneous rheology, it is possible to observe modulation of rolling in more complicated ways. Such potential modulation of rolling in rheologically heterogenous environments, when combined

with the effects of biochemicals, may also result in other unknown navigational strategies with improved benefits for the sperm's search for the oocyte. We explored sperm motion in quiescent reservoirs because we intended to minimize the effect of external fluid flow and solely focus on sperm chemokinetic response. However, external fluid flows can modulate sperm motion in the absence of chemokinetic stimuli. More studies are needed to identify how external fluid flows combined with chemokinesis shape sperm motion dynamically. We speculate that external fluid flows may regulate persistence in the hyperactive phase (as observed in bacterial chemotaxis [2]) or exert a drift in the chiral phase, and thereby contribute to the sperm navigation within the FRT.

Although these results show the ability of sperm to exhibit different phases of motion, regulation of each phase, and the transitions between phases, may not be controlled solely by sperm, but rather by significant contributions from the FRT. Therefore, we speculate the existence of a selection strategy during which, the biphasic chemokinesis we have observed is optimized by FRT only for sperm that can respond appropriately to the rheology, biochemical and physical attributes presented and find the target. In an evolutionary context, this speculation connects the literature on sperm-FRT coevolution [14], and postcopulatory sexual selection [62,63], to the current efforts on optimal search strategies.

M. Z. thanks Christina Kurzthaler, Olivier Bénichou, and Howard Stone for insightful discussions. We also thank the anonymous referees for their constructive criticism. This work was performed in part at the Cornell NanoScale Facility, a member of the National Nanotechnology Coordinated Infrastructure (NNCI), which is supported by the National Science Foundation (Grant NNCI-2025233).

\*Corresponding author.

alireza@cornell.edu

- [1] H. Mattingly, K. Kamino, B. Machta, and T. Emonet, *Escherichia coli* chemotaxis is information limited, *Nat. Phys.*, **17**, 1426 (2021).
- [2] P. de Anna, A. A. Pahlavan, Y. Yawata, R. Stocker, and R. Juanes, Chemotaxis under flow disorder shapes microbial dispersion in porous media, *Nat. Phys.* **17**, 68 (2021).
- [3] T. Bhattacharjee, D. B. Amchin, J. A. Ott, F. Kratz, and S. S. Datta, Chemotactic migration of bacteria in porous media, *Biophys. J.* **120**, 3483 (2021).
- [4] A. Gosztolai and M. Barahona, Cellular memory enhances bacterial chemotactic navigation in rugged environments, *Commun. Phys.* **3**, 47 (2020).
- [5] T. Bhattacharjee and S. S. Datta, Bacterial hopping and trapping in porous media, *Nat. Commun.* **10**, 2057 (2019).
- [6] J. W. Griffith, C. L. Sokol, and A. D. Luster, Chemokines and chemokine receptors: Positioning cells for host defense and immunity, *Annu. Rev. Immunol.* **32**, 659 (2014).
- [7] T. H. Harris, E. J. Banigan, D. A. Christian, C. Konradt, E. D. Tait Wojno, K. Norose, E. H. Wilson, B. John, W. Weninger, and A. D. Luster, Generalized Lévy walks and the role of chemokines in migration of effector CD8+ T cells, *Nature (London)* **486**, 545 (2012).
- [8] D. Masopust and J. M. Schenkel, The integration of T cell migration, differentiation and function, *Nat. Rev. Immunol.* **13**, 309 (2013).
- [9] C. M. Witt, S. Raychaudhuri, B. Schaefer, A. K. Chakraborty, and E. A. Robey, Directed migration of positively selected thymocytes visualized in real time, *PLoS Biol.* **3**, e160 (2005).
- [10] M. Eisenbach and L. C. Giojalas, Sperm guidance in mammals—An unpaved road to the egg, *Nat. Rev. Mol. Cell Biol.* **7**, 276 (2006).
- [11] D. Sakkas, M. Ramalingam, N. Garrido, and C. L. Barratt, Sperm selection in natural conception: What can we learn from Mother Nature to improve assisted reproduction outcomes?, *Human Reprod. Update* **21**, 711 (2015).
- [12] C.-K. Tung and S. S. Suarez, Co-adaptation of physical attributes of the mammalian female reproductive tract and sperm to facilitate fertilization, *Cells* **10**, 1297 (2021).
- [13] D. Miller, M. Brinkworth, and D. Iles, Paternal DNA packaging in spermatozoa: More than the sum of its parts? DNA, histones, protamines and epigenetics, *Reproduction* **139**, 287 (2010).
- [14] D. M. Higginson, K. B. Miller, K. A. Segraves, and S. Pitnick, Female reproductive tract form drives the evolution of complex sperm morphology, *Proc. Natl. Acad. Sci. U.S.A.* **109**, 4538 (2012).
- [15] C. Tung, C. Lin, B. Harvey, A. G. Fiore, F. Ardon, M. Wu, and S. S. Suarez, Fluid viscoelasticity promotes collective swimming of sperm, *Sci. Rep.* **7**, 3152 (2017).
- [16] K. Ishimoto and E. A. Gaffney, Hydrodynamic clustering of human sperm in viscoelastic fluids, *Sci. Rep.* **8**, 15600 (2018).
- [17] V. Kantsler, J. Dunkel, M. Blayney, and R. E. Goldstein, Rheotaxis facilitates upstream navigation of mammalian sperm cells, *eLife* **3**, e02403 (2014).
- [18] K. Miki and D. E. Clapham, Rheotaxis guides mammalian sperm, *Curr. Biol.* **23**, 443 (2013).
- [19] M. Zaferani, S. H. Cheong, and A. Abbaspourrad, Rheotaxis-based separation of sperm with progressive motility using a microfluidic corral system, *Proc. Natl. Acad. Sci. U.S.A.* **115**, 8272 (2018).
- [20] C. Tung, F. Ardon, A. Roy, D. L. Koch, S. S. Suarez, and M. Wu, Emergence of Upstream Swimming via a Hydrodynamic Transition, *Phys. Rev. Lett.* **114**, 108102 (2015).
- [21] C. Tung, L. Hu, A. G. Fiore, F. Ardon, D. G. Hickman, R. O. Gilbert, S. S. Suarez, and M. Wu, Microgrooves and fluid flows provide preferential passageways for sperm over pathogen *Trichomonas foetus*, *Proc. Natl. Acad. Sci. U.S.A.* **112**, 5431 (2015).
- [22] A. Bukatin, I. Kukhtevich, N. Stoop, J. Dunkel, and V. Kantsler, Bimodal rheotactic behavior reflects flagellar beat asymmetry in human sperm cells, *Proc. Natl. Acad. Sci. U.S.A.* **112**, 52 (2015).
- [23] P. Denissenko, V. Kantsler, D. J. Smith, and J. Kirkman-Brown, Human spermatozoa migration in microchannels reveals boundary-following navigation, *Proc. Natl. Acad. Sci. U.S.A.* **109**, 8007 (2012).

- [24] M. Zaferani, G. D. Palermo, and A. Abbaspourrad, Structures of a microchannel impose fierce competition to select for highly motile sperm, *Sci. Adv.* **5**, eaav2111 (2019).
- [25] J. Elgeti, U. B. Kaupp, and G. Gompper, Hydrodynamics of sperm cells near surfaces, *Biophys. J.* **99**, 1018 (2010).
- [26] S. Rode, J. Elgeti, and G. Gompper, Sperm motility in modulated microchannels, *New J. Phys.* **21**, 013016 (2019).
- [27] A. Guidobaldi, Y. Jeyaram, I. Berdakin, V. V. Moshchalkov, C. A. Condat, V. I. Marconi, L. Giojalas, and A. V. Silhanek, Geometrical guidance and trapping transition of human sperm cells, *Phys. Rev. E* **89**, 032720 (2014).
- [28] S. S. Suarez, Control of hyperactivation in sperm, *Human Reprod. Update* **14**, 647 (2008).
- [29] S. Suarez and H. Ho, Hyperactivated motility in sperm, *Reprod. Domest. Anim.* **38**, 119 (2003).
- [30] S. S. SUAREZ, Hyperactivated motility in sperm, *J. Androl.* **17**, 331 (1996).
- [31] A. E. Carlson, R. E. Westenbroek, T. Quill, D. Ren, D. E. Clapham, B. Hille, D. L. Garbers, and D. F. Babcock, CatSper1 required for evoked  $\text{Ca}^{2+}$  entry and control of flagellar function in sperm, *Proc. Natl. Acad. Sci. U.S.A.* **100**, 14864 (2003).
- [32] J.-J. Chung, B. Navarro, G. Krapivinsky, L. Krapivinsky, and D. E. Clapham, A novel gene required for male fertility and functional CATSPER channel formation in spermatozoa, *Nat. Commun.* **2**, 153 (2011).
- [33] H. Qi, M. M. Moran, B. Navarro, J. A. Chong, G. Krapivinsky, L. Krapivinsky, Y. Kirichok, I. S. Ramsey, T. A. Quill, and D. E. Clapham, All four CatSper ion channel proteins are required for male fertility and sperm cell hyperactivated motility, *Proc. Natl. Acad. Sci. U.S.A.* **104**, 1219 (2007).
- [34] T. A. Quill, S. A. Sugden, K. L. Rossi, L. K. Doolittle, R. E. Hammer, and D. L. Garbers, Hyperactivated sperm motility driven by CatSper2 is required for fertilization, *Proc. Natl. Acad. Sci. U.S.A.* **100**, 14869 (2003).
- [35] T. Strünker, N. Goodwin, C. Brenker, N. D. Kashikar, I. Weyand, R. Seifert, and U. B. Kaupp, The CatSper channel mediates progesterone-induced  $\text{Ca}^{2+}$  influx in human sperm, *Nature (London)* **471**, 382 (2011).
- [36] B. Marquez and S. S. Suarez, Bovine sperm hyperactivation is promoted by alkaline-stimulated  $\text{Ca}^{2+}$  influx, *Biol. Reprod.* **76**, 660 (2007).
- [37] J.-J. Chung, S.-H. Shim, R. A. Everley, S. P. Gygi, X. Zhuang, and D. E. Clapham, Structurally distinct  $\text{Ca}^{2+}$  signaling domains of sperm flagella orchestrate tyrosine phosphorylation and motility, *Cell* **157**, 808 (2014).
- [38] P. V. Lishko, Y. Kirichok, D. Ren, B. Navarro, J.-J. Chung, and D. E. Clapham, The control of male fertility by spermatozoan ion channels, *Annu. Rev. Physiol.* **74**, 453 (2012).
- [39] R. Yanagimachi, The movement of golden hamster spermatozoa before and after capacitation, *Reproduction* **23**, 193 (1970).
- [40] M. Zaferani, S. S. Suarez, and A. Abbaspourrad, Mammalian sperm hyperactivation regulates navigation via physical boundaries and promotes pseudo-chemotaxis, *Proc. Natl. Acad. Sci. U.S.A.* **118** (44), e2107500118 (2021).
- [41] See Supplemental Material at <http://link.aps.org/supplemental/10.1103/PhysRevLett.130.248401> for detailed information about methods used in this Letter.
- [42] B. Navarro, Y. Kirichok, and D. E. Clapham, KSper, a pH-sensitive  $\text{K}^+$  current that controls sperm membrane potential, *Proc. Natl. Acad. Sci. U.S.A.* **104**, 7688 (2007).
- [43] M. Finkelstein, N. Etkovitz, and H. Breitbart,  $\text{Ca}^{2+}$  signaling in mammalian spermatozoa, *Mol. Cell. Endocrinol.* **516**, 110953 (2020).
- [44] R. Ma, G. S. Klindt, I. H. Riedel-Kruse, F. Jülicher, and B. M. Friedrich, Active Phase and Amplitude Fluctuations of Flagellar Beating, *Phys. Rev. Lett.* **113**, 048101 (2014).
- [45] C. Kurtzthaler and T. Franosch, Intermediate scattering function of an anisotropic Brownian circle swimmer, *Soft Matter* **13**, 6396 (2017).
- [46] B. Friedrich and F. Jülicher, The stochastic dance of circling sperm cells: Sperm chemotaxis in the plane, *New J. Phys.* **10**, 123025 (2008).
- [47] E. Perez Ipiña, S. Otte, R. Pontier-Bres, D. Czerucka, and F. Peruani, Bacteria display optimal transport near surfaces, *Nat. Phys.* **15**, 610 (2019).
- [48] S. Ebbens, R. A. L. Jones, A. J. Ryan, R. Golestanian, and J. R. Howse, Self-assembled autonomous runners and tumblers, *Phys. Rev. E* **82**, 015304(R) (2010).
- [49] D. F. Babcock, P. M. Wandernoth, and G. Wennemuth, Episodic rolling and transient attachments create diversity in sperm swimming behavior, *BMC Biol.* **12**, 67 (2014).
- [50] M. Zaferani, F. Javi, A. Mokhtare, P. Li, and A. Abbaspourrad, Rolling controls sperm navigation in response to the dynamic rheological properties of the environment, *eLife* **10**, e68693 (2021).
- [51] S. Gadadhar *et al.*, Tubulin glycylation controls axonemal dynein activity, flagellar beat, and male fertility, *Science* **371**, eabd4914 (2021).
- [52] S. Kamdar, S. Shin, P. Leishangthem, L. F. Francis, X. Xu, and X. Cheng, The colloidal nature of complex fluids enhances bacterial motility, *Nature (London)* **603**, 819 (2022).
- [53] J. Elgeti, R. G. Winkler, and G. Gompper, Physics of microswimmers—Single particle motion and collective behavior: A review, *Rep. Prog. Phys.* **78**, 056601 (2015).
- [54] J. R. Howse, R. A. Jones, A. J. Ryan, T. Gough, R. Vafabakhsh, and R. Golestanian, Self-Motile Colloidal Particles: From Directed Propulsion to Random Walk, *Phys. Rev. Lett.* **99**, 048102 (2007).
- [55] B. V. Hokmabad, R. Dey, M. Jalaal, D. Mohanty, M. Almukambetova, K. A. Baldwin, D. Lohse, and C. C. Maass, Emergence of Bimodal Motility in Active Droplets, *Phys. Rev. X* **11**, 011043 (2021).
- [56] A. Izzet, P. G. Moerman, P. Gross, J. Groenewold, A. D. Hollingsworth, J. Bibette, and J. Brujic, Tunable Persistent Random Walk in Swimming Droplets, *Phys. Rev. X* **10**, 021035 (2020).
- [57] Y. Fily and M. C. Marchetti, Athermal Phase Separation of Self-Propelled Particles with No Alignment, *Phys. Rev. Lett.* **108**, 235702 (2012).
- [58] O. Bénichou, C. Loverdo, M. Moreau, and R. Voituriez, Intermittent search strategies, *Rev. Mod. Phys.* **83**, 81 (2011).
- [59] M. Chupeau, O. Bénichou, and R. Voituriez, Cover times of random searches, *Nat. Phys.* **11**, 844 (2015).

- [60] M. R. Raveshi, M. S. Abdul Halim, S. N. Agnihotri, M. K. O'Bryan, A. Neild, and R. Nosrati, Curvature in the reproductive tract alters sperm-surface interactions, *Nat. Commun.* **12**, 3446 (2021).
- [61] B. M. Friedrich and F. Jülicher, Chemotaxis of sperm cells, *Proc. Natl. Acad. Sci. U.S.A.* **104**, 13256 (2007).
- [62] T. R. Birkhead and T. Pizzari, Postcopulatory sexual selection, *Nat. Rev. Genet.* **3**, 262 (2002).
- [63] W. G. Eberhard, Postcopulatory sexual selection: Darwin's omission and its consequences, *Proc. Natl. Acad. Sci. U.S.A.* **106**, 10025 (2009).